Philosophical Magazine
Vol. 92, No. 22, 1 August 2012, 2835–2847

Taylor & Francis
Taylor & Francis Group

Anisotropic interface magnetoresistances in Pt(111)/Co$_n$/Pt(111)

A. Kobs[a]*, S. Heße[a], H.P. Oepen[a] and P. Weinberger[bc]

[a]*Institut für Angewandte Physik, Universität Hamburg, Jungiusstraße 11, 20355 Hamburg, Germany;* [b]*Center for Computational Nanoscience, Seilerstätte 10/22, Vienna, A1010, Austria;* [c]*Department of Physics, New York University, 4 Washington Place, New York 10003, USA*

(*Received 3 November 2011; final version received 8 March 2012*)

It is shown in terms of a fully relativistic spin-polarized *ab initio*-type approach that in Pt/Co/Pt trilayers two types of anisotropic magnetoresistance (AMR) have to be distinguished: an in-plane and an out-of-plane AMR. The obtained results, namely the magnetic field dependence as well as the thickness dependence of both AMR types are in very good agreement with a very recent experimental study, in which the in-plane as well as the out-of-plane AMR was reported for this system. The difference between the two types of AMR is visualized in terms of layer-resolved resistivities. In particular, it is confirmed that the anisotropic interface magnetoresistance (AIMR) introduced in the recent publication mainly originates in the vicinity of the Co/Pt interfaces.

Keywords: magnetoresistance; magnetic effects; magnetic multilayers

1. Introduction

Usually in magnetic multilayer systems when measuring the current in-plane (CIP) anisotropic magnetoresistance (AMR) only the difference in resistivities is recorded that corresponds to (in-plane) orientations of the magnetization being either parallel or perpendicular to the current. Traditionally this difference is expressed as a ratio with respect to one of the terms in the difference. For simple trilayer systems, in which the center layer is a magnetic material, this AMR ratio tends to a constant, namely to the 'bulk'-like value of the spacer material, if the thickness of the spacer grows. In [1] the magnetoresistance (MR) of Pt/Co/Pt films for Co layer thicknesses (d) has been studied for $0.8 \leq d \leq 50$ nm by sweeping the magnetic field in longitudinal, transverse and polar directions and by rotating the samples in a saturation field. Besides the 'usual' AMR, which amounted to about 1.5% at large enough Co thicknesses, it was found that there exists yet another anisotropic MR effect, namely when one of the orientations of the magnetization is kept in-plane and the other is parallel to the surface normal (out-of-plane).

In order to describe on an *ab initio* level both types of MR the in-plane resistivity in Pt/Co/Pt has to be evaluated with respect to different orientations of the magnetic

*Corresponding author. Email: akobs@physnet.uni-hamburg.de

ISSN 1478–6435 print/ISSN 1478–6443 online

http://dx.doi.org/10.1080/14786435.2012.676213
http://www.tandfonline.com

field, which in turn implies that for such a description a relativistic spin-polarized approach has to be applied.

2. Formal definitions

Suppose the magnetic field $\mathbf{M}(\Theta, \Phi)$ points along a general direction where Θ is the angle between $\mathbf{M}(\Theta, \Phi)$ and the z-axis serving as the surface normal, and Φ refers to the angle between the in-plane y-axis and the projection of $\mathbf{M}(\Theta, \Phi)$ into the xy-plane. In particular, for matters of convenience the following short hand notation shall be used,

$$\mathbf{M}_z = \mathbf{M}(0, 0), \quad \mathbf{M}_x = \mathbf{M}(90, 90), \quad \mathbf{M}_y = \mathbf{M}(90, 0),$$

where $\mathbf{M}_x$, $\mathbf{M}_y$ and $\mathbf{M}_z$ denote the special cases where the magnetic field points along the x-, y-, or z-axis.

The in-plane current along the in-plane x-axis with respect to $\mathbf{M}(\Theta, \Phi)$ is given by [2–9]

$$\begin{aligned} j_x(d; \mathbf{M}(\Theta, \Phi)) &= \sum_{i,j=1,n} \sigma_{xx}^{ij}(d; \mathbf{M}(\Theta, \Phi)) E_x^j \\ &\sim E_x \sum_{i,j=1,n} \sigma_{xx}^{ij}(d; \mathbf{M}(\Theta, \Phi)) = E_x \sigma_{xx}(d; \mathbf{M}(\Theta, \Phi)), \end{aligned} \tag{1}$$

where the $\sigma_{xx}^{ij}(d; \mathbf{M}(\Theta, \Phi))$ are the x-like layer-resolved elements of the corresponding conductivity tensor [10,11], d is the thickness of the Co slab and E_x is the electric field. In order to facilitate a comparison with the experimental data in [1] it should be noted that the orientation of $\mathbf{M}$ along the x, y, z axes corresponds to the longitudinal, transverse, and polar geometry, respectively. Accordingly, the following differences of in-plane currents

$$\Delta j_x(d; \mathbf{M}(\Theta, \Phi), \mathbf{M}_y) = j_x(d; \mathbf{M}(\Theta, \Phi)) - j_x(d; \mathbf{M}_y), \tag{2}$$

and difference resistivities [9]

$$\Delta \rho_{xx}(d; \mathbf{M}(\Theta, \Phi), \mathbf{M}_y) = \rho_{xx}(d; \mathbf{M}(\Theta, \Phi)) - \rho_{xx}(d; \mathbf{M}_y), \tag{3}$$

$$\rho_{xx}(d; \mathbf{M}) = \sigma_{xx}(d; \mathbf{M})^{-1}, \tag{4}$$

are evaluated.

3. Note on the temperature dependence of the resistivity

However, in order to compare the theoretical results ($T = 0$ K) with the experimental data (room temperature) first a short note on the role of temperature on the resistivity is needed. At finite temperatures and for a given magnetic field $\mathbf{M}$ the resistivity $R(d; \mathbf{M}, T)$ can be assumed to be of the form [12]

$$R(d; \mathbf{M}, T) = \rho_{e-p}(d; T) + \rho(d; \mathbf{M}, T) + \rho_G(d; \mathbf{M}, T), \tag{5}$$

where the electron–phonon contribution $\rho_{e-p}(d;T)$ clearly is independent of the magnetic configuration, the magnetic resistivity $\rho(d;\mathbf{M},T)$ could include additional contributions arising from the presence of domain walls [13,14], and $\rho_G(d;\mathbf{M},T)$ refers to effects of structural disorder (dislocations, imperfections, gradual structural changes of the underlying parent lattice). Since this kind of contribution cannot be accounted for in a microscopic theoretical description, it will be assumed to be essentially independent of the magnetic configuration, i.e. $\rho_G(d;\mathbf{M},T)\sim\rho_G(d;T)$. Clearly, by calculating difference resistivities the $\rho_{e-p}(d;T)$ and $\rho_G(d;T)$ terms vanish, thus

$$\Delta\rho(d;\mathbf{M},\mathbf{M}',T)\sim\Delta R(d;\mathbf{M},\mathbf{M}',T). \tag{6}$$

Earlier theoretical studies of the temperature dependent magnetic resistivity of bulk-like materials $\rho(\mathbf{M},T)$ were based on Boltzmann transport theory by making use of an *s–d* scattering model Hamiltonian (*s–d* interaction) [15–17], or, applied the two current model of Fert [18–22]. In both cases experimental parameters were used in order to determine $\rho(\mathbf{M},T)$.

In terms of *ab initio*-like descriptions there seems to be, up to now, only a single study [12] of $\rho(\mathbf{M},T)$, namely for bulk Fe and Co, in which use is made of the so-called Disordered Local Moments (DLM) theory. In this theory, originally proposed for finite temperature magnetic properties of bulk-like systems [23–26], and later on for two-dimensional translational invariant systems [27], the 'disorder' of magnetic moments caused by finite temperatures is taken care of by means of ensemble averages over orientational configurations in terms of a generalized Coherent Potential Approximation (CPA). For further details and explanations, see also [10]. These averages have to be performed for each given temperature, the results of which then enter as inputs in the Kubo equation [12]. It should be noted that presently even the generalized CPA is restricted to a perfect underlying lattice.

Although, in principle, treating finite temperature effects *ab initio*-like is possible, it is obviously quite demanding even for a bulk system corresponding to a simple lattice. However, since recent experimental results of a Pt/Co/Pt sandwich with a Co thickness of 6 nm show only a slight temperature dependence of $\Delta\rho(\mathbf{M},\mathbf{M}',T)$ in the temperature range of 4.2 K $\leq T \leq$ 295 K [28], namely

$$\left|\frac{\Delta\rho(\mathbf{M},\mathbf{M}',T)-\Delta\rho(\mathbf{M},\mathbf{M}',T_0)}{\Delta\rho(\mathbf{M},\mathbf{M}',T_0)}\right| < 10\%,$$
$$\forall\,(\mathbf{M},\mathbf{M}'),\quad T_0 = 4.2\mathrm{K},$$

a comparison between the experimental data in Ref. [1] and the theoretical results seems to be justified.

4. Computational details

All (self-consistent) *ab initio* electronic structure calculations for Pt(111)/Co_n/Pt(111), $n \leq 90$ ML being the fcc Co (111) thickness in monolayers (ML), were performed for a uniform direction of the magnetization pointing along the surface normal in terms of the spin-polarized (fully) relativistic screened Korringa–Kohn–Rostoker method [10].

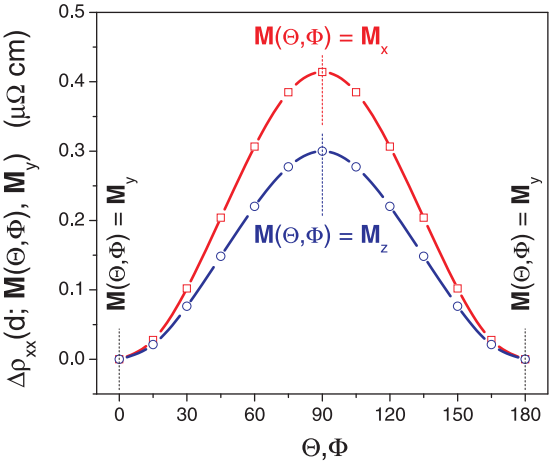

Figure 1. Pt(111)/Co_{27}/Pt(111). Angle dependence of the difference resistivities in Equation (3).

The free energies were obtained (at zero temperature) in terms of the magnetic force theorem [11]; the electronic transport properties were evaluated by means of the fully relativistic Kubo–Greenwood [11] equation, by making use of complex Fermi energies $\mathcal{E}_F = E_F + i\delta$ and subsequent numerical continuation to the real energy axis. In all calculations a maximum angular quantum number of two [10], the density functional parametrization of [29] and the atomic sphere approximation (ASA) were used.

Since per definition the current has to be independent of the choice of the coordinate system, the difference $e(d) = \rho_{xx}(d; \mathbf{M}_x) - \rho_{yy}(d; \mathbf{M}_y)$ ought to be zero for all d and is therefore most suitable to check the numerical accuracy of the calculated resistivities. It turned out that in the regime of $4 \leq d \leq 20$ nm on average a maximal numerical error of 0.03 μΩ cm has to be taken into account.

5. Results

5.1. *Pt(111)/Co_{27}/Pt(111)*

5.1.1. *Angle dependent difference resistivities*

Since in the experimental study detailed results are shown for a Co thickness of 6 nm, for matters of comparison in Figure 1 for a Co thickness of 27 ML (~5.44 nm) the angle dependence of the difference resistivities $\Delta\rho_{xx}(d; \mathbf{M}(\Theta, 0), \mathbf{M}_y)$ and $\Delta\rho_{xx}(d; \mathbf{M}(90, \Phi), \mathbf{M}_y)$ are displayed for Θ, $\Phi \in [0, 180]$. The theoretical curves confirm the experimentally found functional dependence of the difference resistivities, namely the $\cos^2$ dependence with respect to the varied angles. Furthermore, the theoretical values of $\Delta\rho_{xx}(d; \mathbf{M}_z, \mathbf{M}_y)$ and $\Delta\rho_{xx}(d; \mathbf{M}_x, \mathbf{M}_y)$ are in very good agreement with their experimental complements: Experimentally, it is found that $\Delta\rho_{xx}(d; \mathbf{M}_z, \mathbf{M}_y)$ is about 0.19 μΩ cm, while in Figure 1 it is 0.3 μΩ cm. The difference $\Delta\rho_{xx}(d; \mathbf{M}_x, \mathbf{M}_y)$ amounts in the experimental study to about 0.29 μΩ cm, in the theoretical study to 0.41 μΩ cm.

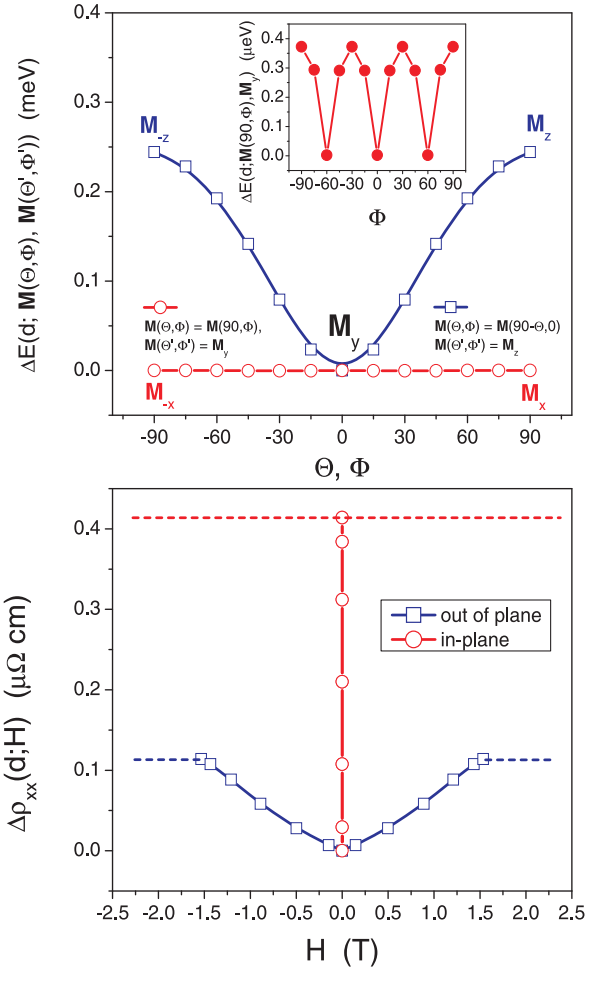

Figure 2. Pt(111)/Co_{27}/Pt(111). Top: angle dependence of the out-of-plane and the in-plane free energy, see Equation (7). The inset shows the angle dependence of the in-plane free energy on a μeV scale. Bottom: out-of-plane and in-plane difference resistivities, see Equation (3), versus applied magnetic field.

5.1.2. *Field dependence of the difference resistivities*

As the experimental transport measurements were carried out in the presence of an external field, in the upper half of Figure 2, the angle dependence of the free energy $\Delta E(d; \mathbf{M}(\Theta, \Phi), \mathbf{M}(\Theta', \Phi'))$,

$$\Delta E(d; \mathbf{M}(\Theta, \Phi), \mathbf{M}(\Theta', \Phi')) = E(d; \mathbf{M}(\Theta, \Phi)) - E(d; \mathbf{M}(\Theta', \Phi')), \tag{7}$$

is displayed for a Co thickness of 27 ML. It should be noted that in Equation (7) $\Delta E(d; \mathbf{M}(\Theta, \Phi), \mathbf{M}(\Theta', \Phi'))$ is the free energy difference between an orientation of the magnetization specified by Θ and Φ and one corresponding to Θ' and Φ'. For example, $\Delta E(d; \mathbf{M}(90, \Phi), \mathbf{M}_y)$ refers to in-plane changes of the free energy,

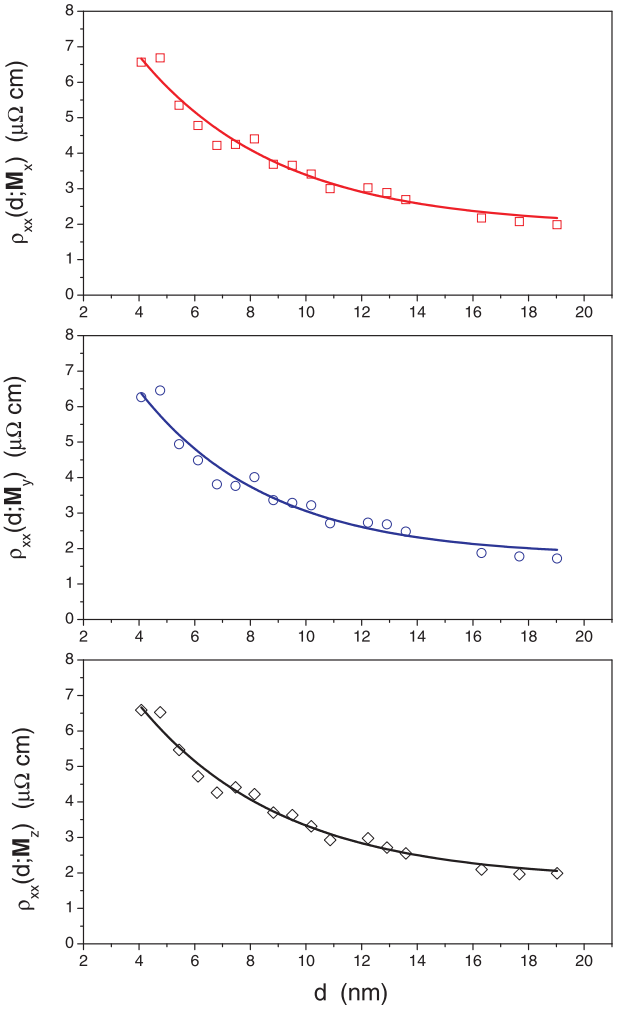

Figure 3. Resistivities $\rho_{xx}(d; \mathbf{M}_x)$ (top), $\rho_{xx}(d; \mathbf{M}_y)$ (middle) and $\rho_{xx}(d; \mathbf{M}_z)$ together with fits (full lines) to a single exponential, see text.

i.e. changes when the orientation of the magnetization rotates within the xy-plane; $\Delta E(d; \mathbf{M}(\Theta, 0), \mathbf{M}_y)$ reflects such changes in the yz-plane, i.e. refers to the angle dependence of the out of plane free energy.

In layered systems such as Pt(111)/Co_n/Pt(111) in-plane anisotropies are usually by orders of magnitude smaller than out-of-plane anisotropies. In the present case it turns out that they are of the order of μeV, see the inset in Figure 2, which in turn corresponds to an external field of a few tens of a mT. It should be noted that since for Pt(111) the two-dimensional rotational symmetry is $\mathcal{C}_3$ the in-plane anisotropy shows minima at $\Phi = 60, 120, 180$. Depending on the type of system out-of-plane free energies amount to about 0.1 to 0.2 meV per interface. The present out-of-plane free energy of 0.114 meV per interface, see also Figures 2 and 5 (in Section 6), is slightly

larger than the corresponding value of 0.091 meV for a free surface of a single Co layer on top of Pt(111) [30].

Since $\Delta E(d;\ \mathbf{M}(\Theta,\Phi),\ \mathbf{M}(\Theta',\Phi'))$ is proportional to the magnitude of the applied external field, in the lower part of Figure 2 $\Delta\rho_{xx}(d;\mathbf{M}(\Theta,\Phi),\mathbf{M}_y)$ is displayed as an implicit function of the corresponding $\Delta E(d;\ \mathbf{M}(\Theta,\Phi),\ \mathbf{M}(\Theta',\Phi'))$. This part of Figure 2 can now be directly compared with the actually measured values.

Experimentally it was found that on the scale of Teslas because of the tiny in-plane anisotropy just mentioned for in-plane fields $\Delta\rho_{xx}(d;\ \mathbf{M}(90,\Phi),\mathbf{M}_y)$ virtually shows no field dependence at all, i.e. at an external field of $H\sim 0$, two values of $\rho_{xx}(d;\mathbf{M})$ exist, namely $\rho_{xx}(d;\mathbf{M}_x)$ and $\rho_{xx}(d;\mathbf{M}_y)$. The external field necessary to move in the experiment $\mathbf{M}_y$ to $\mathbf{M}_z$ is about 1.3 T (saturation field) [1], which has to be compared with a corresponding theoretical value of about 1.5 T.

It is important to note that once the magnetization is oriented along **z**, there is no further ferromagnetic state higher in energy that can be reached by increasing the external field, i.e. $\Delta\rho_{xx}(d;\mathbf{H})$ remains constant (indicated in Figure 2 by dashed lines).

5.2. *Thickness dependence of the difference resistivities*

Before turning to the thickness dependence of the difference resistivities one has to consider that in the experiment all oscillations of the resistivity with respect to the thickness are 'wiped out' because of structural and thermal disorder. In order to 'wipe out artificially' these oscillations in the $\rho_{xx}(d;\mathbf{M})$ with respect to d, in Figure 3 these functions are fitted in the interval $4 \le d \le 20$ nm to single exponentials (full line), the fitted functions being denoted in the following by $\rho_{xx}^{\mathrm{fit}}(d;\mathbf{M})$.

From Figure 4a one can see that the $\Delta\rho_{xx}^{\mathrm{fit}}(d;\mathbf{M}_\nu,\mathbf{M}_y), \nu = x, z,$ namely the difference resistivities based on the fits mentioned above, apparently show the same size as their experimental counterparts, $\Delta\rho_{xx}^{\mathrm{exp}}(d;\mathbf{M}_\nu,\mathbf{M}_y)$. It is quite assuring that in the whole thickness range, even at a Co thickness of about 20 nm (about 100 ML of Co), the $\Delta\rho_{xx}^{\mathrm{fit}}(d;\mathbf{M}_\nu,\mathbf{M}_y)$, $\nu = x, z$ differ from their experimental counterparts by less than about 0.2 μΩ cm while the curves $\Delta\rho_{xx}^{\mathrm{fit}}(d;\mathbf{M}_z,\mathbf{M}_y)$ and $\Delta\rho_{xx}^{\mathrm{exp}}(d;\mathbf{M}_z,\mathbf{M}_y)$ reveal additionally a very similar dependence on thickness (dashed lines in Figure 4a). $\Delta\rho_{xx}^{\mathrm{fit}}(d;\mathbf{M}_x,\mathbf{M}_y)$, however, shows an exponential decay at large thicknesses in contrast to $\Delta\rho_{xx}^{\mathrm{exp}}(d;\mathbf{M}_x,\mathbf{M}_y)$ (solid lines in Figure 4a). The different asymptotic behavior becomes more obvious when comparing respective functions d times $\Delta\rho_{xx}(d;\mathbf{M}_\nu,\mathbf{M}_y)$, see Figure 4b. It is instructive to consider the general functional behavior in the case d, the Co thickness, is sufficiently large such that

$$d\Delta\rho_{xx}(d;\mathbf{M}_\nu,\mathbf{M}_y) = \begin{cases} a + kd : \text{linear increase} \\ Ae^{-kd} : \text{exponential decay} \\ b \ : \text{constant} \end{cases}$$

with A, a, b and k being appropriate constants, and therefore

$$\lim_{\mathrm{d}\to\infty}\left(\rho_{xx}(d;\mathbf{M}_\nu) - \rho_{xx}(d;\mathbf{M}_y)\right) = \begin{cases} k : \text{linear increase} \\ 0 : \text{otherwise} \end{cases}$$

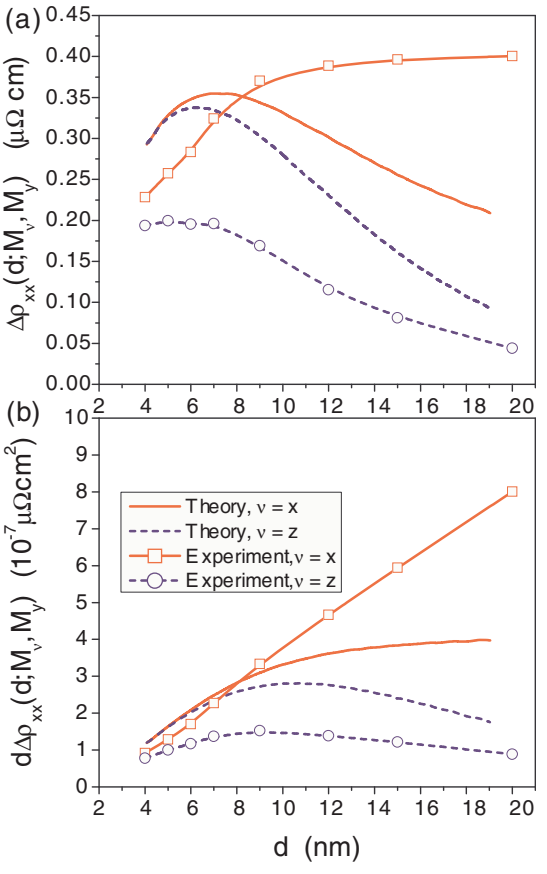

Figure 4. $\Delta\rho_{xx}^{\mathrm{fit}}(d;\mathbf{M}_v,\mathbf{M}_y)$, $v = x, z$, versus the thickness of the Co slab. Also displayed are the corresponding experimental data.

which is the normal behavior expected for an isotropic bulk material. The different asymptotic behavior of $\Delta\rho_{xx}^{\mathrm{fit}}(d;\mathbf{M}_x,\mathbf{M}_y)$ and $\Delta\rho_{xx}^{\mathrm{exp}}(d;\mathbf{M}_x,\mathbf{M}_y)$ is a consequence of the different sample quality. In the calculations a perfect crystal structure is assumed which should merge into a zero resistivity in the limit of infinite Co thickness

$$\lim_{\mathrm{d}\to\infty}\rho_{xx}^{\mathrm{fit}}(d;\mathbf{M}_v)=0$$

at $T=0\,\mathrm{K}$. Consequently, this implies that $\Delta\rho_{xx}^{\mathrm{fit}}(d;\mathbf{M}_x,\mathbf{M}_y)$ is dropping towards zero, which is the case as can be seen in Figure 4a. In the experiment, however, the trend of $\Delta\rho_{xx}^{\mathrm{exp}}(d;\mathbf{M}_x,\mathbf{M}_y)$ for large d has to be interpreted in the framework of defects in the measured films. Imperfections of the structure and thermal excitations give the major contributions to the bulk AMR. This causes $\Delta\rho_{xx}^{\mathrm{exp}}(d;\mathbf{M}_x,\mathbf{M}_y)$ to merge to a constant value >0.

For instance, in the case of Co films it was shown [31] that an extrapolation of the AMR ratio to very low temperatures (4.2 K) depends very much on the sample preparation. The apparently good agreement at lower thicknesses between theory

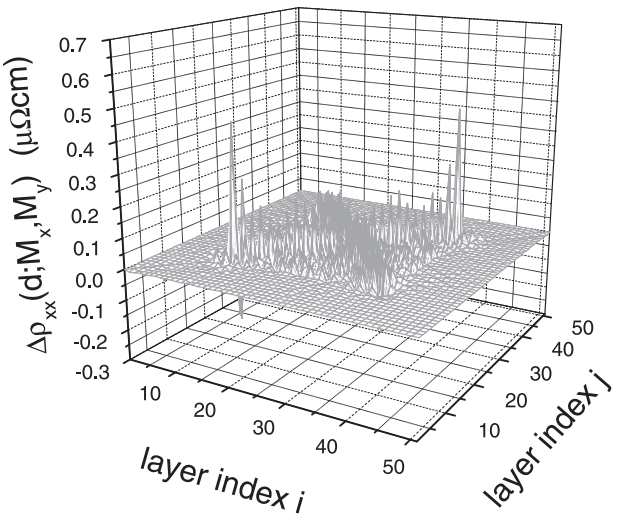

Figure 5. Pt(111)/Co_{27} /Pt(111). Layer-resolved difference resistivity $\Delta\rho^{ij}_{xx}(d; M_x, M_y)$.

and experiment is due to the fact that in the theory an interface contribution to the AMR is found that was not resolved in the experiments which again might be a result of the imperfections of the multilayers, like e.g. interdiffusion or intermixing.

6. Discussion

Most of the physical phenomena discussed above are caused by the Pt/Co interfaces. In order to illustrate these interface effects in detail the $\sigma^{ij}_{xx}(d; \mathbf{M})$ matrix, see Equation (1), can be inverted,

$$\rho^{ij}_{xx}(d; \mathbf{M}) = [\sigma_{xx}(d; \mathbf{M})]^{-1}_{ij}, \tag{8}$$

and the following difference be formed

$$\Delta\rho^{ij}_{xx}(d; \mathbf{M}_\nu, \mathbf{M}_y) = \rho^{ij}_{xx}(d; \mathbf{M}_\nu,) - \rho^{ij}_{xx}(d; \mathbf{M}_y), \tag{9}$$

where it should be recalled that i and j denote atomic layers and $\nu = x, z$. Note that of course only the sum over all $\Delta\rho^{ij}_{xx}(d; \mathbf{M}_\nu, \mathbf{M}_y)$ has a well-defined physical meaning. Clearly, by definition the current is a non-local quantity, however, when displaying difference resistivities not only the contribution of the semi-infinite parts of the leads essentially cancels out, but also the effect of orientation of the magnetization becomes visible mostly in terms of the on-site elements. In using a three-dimensional visualization by displaying $\Delta\rho^{ij}_{xx}(d; \mathbf{M}_\nu, \mathbf{M}_y)$ versus i and j one obtains a very detailed view of the spacial origin of the two different kinds of difference resistivity, $\Delta\rho_{xx}(d; \mathbf{M}_x, \mathbf{M}_y)$ and $\Delta\rho_{xx}(d; \mathbf{M}_z, \mathbf{M}_y)$. In Figures 5 and 6 the $\Delta\rho^{ij}_{xx}(d; \mathbf{M}_x, \mathbf{M}_y)$ and $\Delta\rho^{ij}_{xx}(d; \mathbf{M}_z, \mathbf{M}_y)$ are shown for 27 Co layers ($d = 5.44$ nm), in Figures 7 and 8 for 90 Co layers ($d = 19.03$ nm). In all four figures the flat part ('rim') corresponds to Pt. As one can see from Figures 5 and 6 in the case of 27 Co layers the Pt/Co interfaces

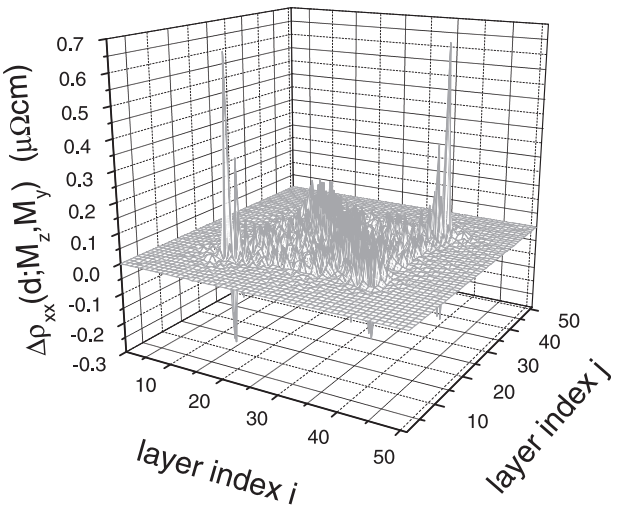

Figure 6. Pt(111)/Co_{27}/Pt(111). Layer-resolved difference resistivity $\Delta\rho_{xx}^{ij}(d; \mathbf{M}_z, \mathbf{M}_y)$.

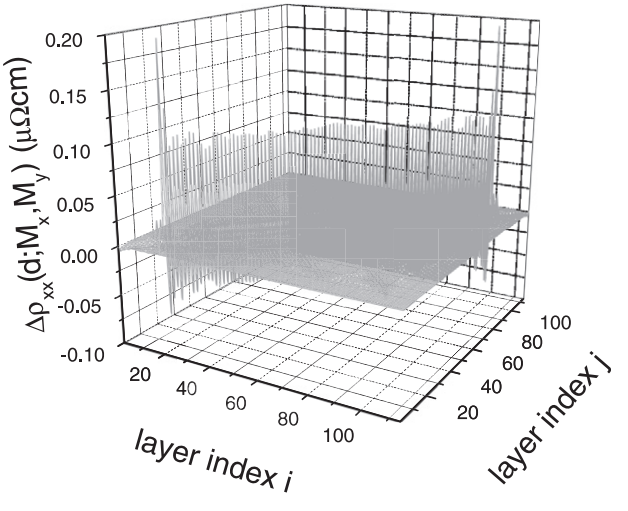

Figure 7. Pt(111)/Co_{90} /Pt(111). Layer-resolved difference resistivity $\Delta\rho_{xx}^{ij}(d; \mathbf{M}_x, \mathbf{M}_y)$.

contribute substantially to both difference resistivities, whereas for 90 Co layers there is a striking difference between $\Delta\rho_{xx}^{ij}(d; \mathbf{M}_x, \mathbf{M}_y)$ and $\Delta\rho_{xx}^{ij}(d; \mathbf{M}_z, \mathbf{M}_y)$: if the magnetization points along the z-direction the contributions from the Pt/Co interfaces vanish almost completely. This difference for reasonably thick Co slabs explains rather well the different thickness dependence of $\Delta\rho_{xx}^{\mathrm{fit}}(d; \mathbf{M}_x, \mathbf{M}_y)$ and $\Delta\rho_{xx}^{\mathrm{fit}}(d; \mathbf{M}_z, \mathbf{M}_y)$ shown in Figure 4. The non-locality of the current can be seen best even in the case of difference resistivities from Figure 5 considering for example the

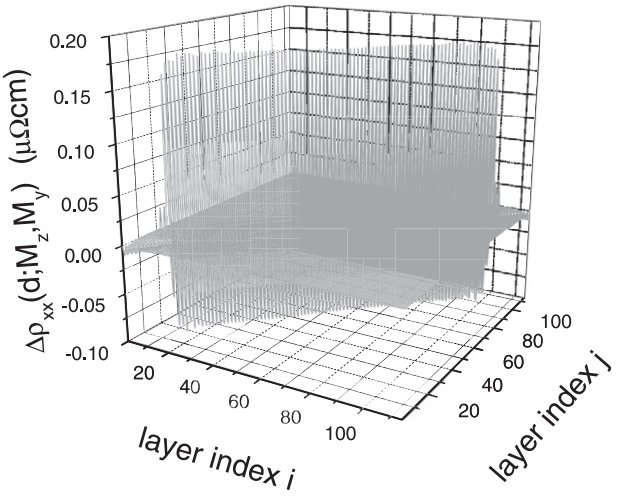

Figure 8. Pt(111)/Co_{90} /Pt(111). Layer-resolved difference resistivity $\Delta\rho_{xx}^{ij}(d;\mathbf{M}_z,\mathbf{M}_y)$.

case of the first Co layer ($i=13$, $1\leq j\leq 51$): even the very last Co-like element, $j=51$, yields a non-vanishing contribution to the total difference resistivity. Figures 5–8 re-enforce very strongly the fact that although the total system consisting of the Pt leads and the Co film is macroscopic, the measured property is caused by a nanostructured part of it.

7. Conclusion

So far, the experimental results of [1] concerning $\Delta\rho_{xx}(d;\mathbf{M}_z,\mathbf{M}_y)$ not only have been confirmed, but also, despite the fact that rather small differences in resistivities had to be described, a reasonably good agreement between experiment and theory was found. Most importantly, as the lower part of Figure 2 exemplarily reveals, at each given thickness d both $\Delta\rho_{xx}(d;\mathbf{M}(\Theta,\Phi),\mathbf{M}_y)$ exhibit a completely different response with respect to the applied field. Clearly enough by dividing respective difference resistivities by $\rho_{xx}(d;\mathbf{M}_y)$ (or $\rho_{xx}(d;\mathbf{M}_y,T)$) one obtains two different kinds of anisotropic magnetoresistance ratios, the novel fact that was claimed in [1]. In particular Figures 7 and 8 support this claim. The theoretical treatment, however, predicts an interface contribution to $\Delta\rho_{xx}(d;\mathbf{M}_x,\mathbf{M}_y)$, i.e. the conventional AMR, which has not been detected experimentally so far. It should be noted that all theoretical results are based on Density Functional Theory (DFT) and on fully relativistic multiple scattering theory in terms of the screened Korringa–Kohn–Rostoker method and a corresponding Kubo–Greenwood equation of electric transport, i.e. are entirely *ab initio*-like. The only assumption besides the choice of a particular parametrization of DFT concerns the underlying lattice, which refers to that in the left and right semi-infinite system, namely that in fcc Pt(111). In principle, even (layer-) relaxation effects can approximately be taken into account [32] if it turns out that there is strong experimental evidence for such effects.

Acknowledgements

Financial support via SFB 668 and Landesexzellenzinitiative Hamburg is gratefully acknowledged.

References

[1] A. Kobs, S. Heße, W. Kreuzpainter, G. Winkler, D. Lott, P. Weinberger, A. Schreyer and H.P. Oepen, Phys. Rev. Lett. 106 (2011) p.217207.
[2] R. Kubo, M. Toda and N. Hashitsume, *Statistical Physics II: Non-equilibrium Statistical Mechanics*, Springer, Berlin, 1985.
[3] R. Kubo, J. Phys. Soc. Jpn. 12 (1957) p. 570.
[4] J.M. Luttinger, *Transport theory*, in *Mathematical Methods in Solid State and Superfluid Theory*, R.C. Clark and G.H. Derrick, eds., Chap. 4, Oliver and Boyd, Edinburgh, 1969, p.157.
[5] D.A. Greenwood, Proc. Phys. Soc. London 71 (1958) p.585.
[6] W.H. Butler, Phys. Rev. B 31 (1985) p.3260.
[7] P.M. Levy, *Giant magnetoresistance in magnetic layered and granular materials*, in *Solid State Physics*, H. Ehrenreich and D. Turnbull, eds., Chap. 12, Vol. 47, Academic Press, Cambridge, MA, 1994, p.367.
[8] P.M. Levy and I. Mertig, *Theory of giant magnetoresistance*, in *Spin-dependent Transport in Magnetic Nanostructures*, T. Shinjo and S. Maekawa, eds., Chap. 2, Gordon and Breach Science Publisher, New York, 2001, p.95.
[9] P. Weinberger, Phys. Rep. 377 (2003) p.281.
[10] J. Zabloudil, R. Hammerling, L. Szunyogh and P. Weinberger, *Electron Scattering in Solid Matter*, Springer, New York, 2004.
[11] P. Weinberger, *Magnetic Anisotropies in Nanstructured Matter*, CRC, Boca Raton, 2008.
[12] A. Buruzs, L. Szunyogh and P. Weinberger, Phil. Mag. 88 (2008) p.2615.
[13] P. Weinberger, Phys. Rev. Lett. 100 (2008) p.017201.
[14] P. Weinberger, Phys. Rev. B 78 (2008) p.172404.
[15] D.A. Goodings, Phys. Rev. 132 (1963) p.542.
[16] B. Raquet, M. Viret, E. Sondergard, O. Cespedes and R. Mamy, Phys. Rev. B 66 (2002) p.024433.
[17] B. Raquet, M. Viret, J. Broto, E. Sondergard, O. Cespedes and R. Mamy, J. Appl. Phys. 91 (2002) p.8129.
[18] A. Fert and I. Campbell, Phys. Rev. Lett. 21 (1968) p.1190.
[19] A. Fert and I. Campbell, J. Phys. F: Met. Phys. 6 (1976) p.849.
[20] A. Fert, J. Phys. F: Met. Phys. 1 (1971) p.L42.
[21] A. Fert, J. Phys. C: Solid State Phys. 2 (1969) p.1784.
[22] D.L. Mills, A. Fert and I. Campbell, Phys. Rev. B 4 (1971) p.196.
[23] B.L. Györffy, A.J. Pindor, J.B. Staunton, G.M. Stocks and H. Winter, J. Phys. F 15 (1985) p.1337.
[24] S.S.A. Razee, J.B. Staunton, L. Szunyogh and B.L. Györffy, Phys. Rev. B 66 (2002) p.094415.
[25] J.B. Staunton, S. Ostanin, S.S.A. Razee, B.L. Györffy, L. Szunyogh, B. Ginatempo and E. Bruno, Phys. Rev. Lett. 93 (2004) p.257204.
[26] J.B. Staunton, L. Szunyogh, Á. Buruzs, B.L. Györffy, S. Ostanin and L. Udvardi, Phys. Rev. B 74 (2006) p.144411.
[27] Á. Buruzs, P. Weinberger, L. Szunyogh, L. Udvardi, P.I. Chleboun, A.M. Fischer and J.B. Staunton, Phys. Rev. B 76 (2007) p.064417.

[28] Private communication, to be published.
[29] S.H. Vosko, L. Wilk and M. Nusair, Can. J. Phys. 58 (1980) p.1200.
[30] P. Weinberger, A. Vernes, L. Szunyogh and J. Zabloudil, Phys. Rev. B 80 (2009) p.075430.
[31] P.P. Freitas, A.A. Gomes, T.R. McGuire and T.S. Plaskett, J. Magn. Magn. Mater. 83 (1990) p.113.
[32] P. Weinberger, Phys. Rev. B 81 (2010) p.184412.